Tanzania Journal of Science 50(2): 347-358, 2024
ISSN 0856-1761, e-ISSN 2507-7961

Image Reconstruction Method Based on Iterative Linear Back Projection and Logistic Forward Solver for Electrical Capacitance Tomography Measurement System

Alfred Mwambela and Josiah Nombo*
Electronics and Telecommunications Engineering Department, University of Dar es Salaam, Tanzania
Received 15 Oct 2023, Revised 20 March 2024, Accepted 23 June 2024Published June 30
**Corresponding author: jpnombo@gmail.com, jpnombo@udsm.ac.tz*
https://dx.doi.org/10.4314/tjs.v50i2.14

Abstract

Image reconstruction is one of the important tasks in the application of electrical capacitance tomography (ECT) systems. Though numerous algorithms have been implemented, it is often challenging to obtain satisfactory images in all imaging regions by the use of a single algorithm due to the soft-field nature of ECT systems. The preferred iterative reconstruction algorithms are highly computationally inefficient. A new iterative reconstruction algorithm is proposed which combine iterative Linear Back Projection and Logistic Regression. In this method, the solution to the ECT forward problem is implemented using logistic regression, whereas the ECT inverse problem is solved using the algebraic reconstruction technique. By doing so, it is possible to obtain high quality images at relatively efficient computational cost. The simulated experimental results shows that the proposed algorithm outperforms the Projected Landweber and Iterative Linear Back Projection in terms of spatial similarity accuracy, quality of reconstruction images, and computational efficiency. There are improvements of 29 % spatial similarity accuracy and 58 % computational cost relative to Iterative Linear Back Projection algorithm. This is significant improvement toward using ECT system for online industrial operations.

Keywords: Electrical Capacitance Tomography; Inverse Problem; Image Reconstruction; Logistic Regression.

Introduction

Tomography imaging is a technique used to construct cross-sectional images from data obtained using tomography systems (Dimas et al. 2024). The fundamental principle of these systems is to determine the component distributions of materials by using data obtained from sensors strategically placed around the process under observation (Rajan and Jose 2022). Among various tomographic imaging, Electrical capacitance tomography (ECT) has gained a considerable attention as a powerful imaging tool in industrial applications because it offers a number of advantages such as a simplified structure, a wide range of applications, lower cost, non-destructive and non-invasive nature, and guaranteed safety (Chowdhury et al. 2022, Li et al. 2023). However, the use of ECT for online industrial process monitoring is challenging due to its “soft field” nature, whereby the sensing field is highly a non-linear function of the permittivity distribution of the material under investigation (Deabes and Jamil Khayyat 2021, Wang and Yang 2021). This non-linearity challenges the establishment of analytical and explicit relationship between measured capacitance data and permittivity distribution.

Therefore, the process of obtaining images from the process under observation using ECT systems is often accomplished using either

single step or iterative methods. Iterative methods are more predominant because they generate images of higher quality from compared to singe step methods but at a higher computational cost (Zheng and Peng 2020). The fundamental principle of iterative methods is based on optimizing a set of objective functions until a stable solution is attained. In most ECT iterative techniques, the sensitivity model is used to find an update of the reconstructed image. The sensitivity model is based on dividing the sensing domain into small pixels, and the capacitance data are obtained as a linear sum of different perturbations composing the overall permittivity distribution. Using this model, forward and inverse solutions are respectively obtained through a linear forward projection (LFP) and linear backward projection (LBP) of the image vector and the capacitance measurement onto the sensitivity matrix (Wajman 2021, Yang et al. 2023). The advantages of sensitivity model are simple implementation and minimum computational cost. However, it provides a relatively poor accurate solution for the non-linear ECT problem, which results into an increased error as the degree of permittivity difference between phases being imaged increases. Therefore, nonlinear iterative solutions are necessary to overcome the limitations.

This work presents a new iterative approach for solving the non-linear forward/inverse problem in soft-field ECT environment using non-linear forward solver. The method uses a nonlinear update of the image vector for the reconstruction process by implementing a logistic regression forward solver and iterative linear back projection technique. The new updating technique eliminates the instability problem usually encountered in linear iterative methods. Experimental results suggest a greater improvement in reconstruction performance of non-linear update when compared with state-of-the-art techniques, such as projected Landweber (Wajman 2021, Yang et al. 2023) and iterative linear back projection. Advantages of combining logistics forward solver and iterative linear back projection techniques to solve both the forward and inverse problems include a better approximation to the forward and inverse non-linear ECT solutions, and an increase in computational speed.

Materials and Methods

ECT Basic Equations

ECT system consists of an array of n electrodes surrounding a pipe or a container. The total number of independent capacitance measurements is given by $\frac{n(n-1)}{2}$, which is equal to the number independent electrode pairs. The measured capacitances are used to reconstruct the permittivity distribution inside the pipe or container which in turn give an image of the cross-section of the process under observation.

This process of reconstructing images involves solving two major computational problems: forward and inverse problems (Hong et al. 2021, Wang and Yang 2021). The forward problem calculates potential distribution from a known permittivity, and hence determines capacitance measurements. The inverse problem calculates permittivity distribution from the measured capacitance data. Results from the inverse problem are normally presented as a visual image, and hence the process is called image reconstruction. The electric potential depends on the permittivity distribution according to the Poisson equation as

$$\nabla[\varepsilon(x,y)\nabla\phi(x,y)] = -\rho(x,y) \qquad (1)$$

where $\varepsilon(x,y)$, $\phi(x,y)$ and $\rho(x,y)$ are respectively, permittivity distribution, electric potential and charge distributions. Equation (1) is a linear partial differential equation in terms of $\phi(x,y)$, the non-linearity in ECT refers to the nonlinear dependency of $\phi(x,y)$ on $\varepsilon(x,y)$. The capacitance between electrode pair, ij, is obtained by

$$C_{ij} = \frac{Q_j}{\Delta V_{ij}}, \qquad (2)$$

where C_{ij} is the mutual capacitance between electrode pair ij, ΔV_{ij} is the potential difference, and Q_j is the charge on the sensing electrode, obtained from Gauss law using

$$Q_j = \oint_{\tau_j} \varepsilon(x,y)\nabla\phi(x,y)\cdot\hat{n}dl, \quad (3)$$

where τ_j is a closed path enclosing the sensing electrode and $\hat{n}$ is the unit vector normal to τ_j. The image reconstruction equation is given by

$$C_{ij} = \frac{1}{V}\iint_{\tau} \varepsilon(x,y)\nabla\phi(x,y)d\tau, \quad (4)$$

and called the ECT model, is normally approximated in matrix form as

$$C \cong SG, \quad (5)$$

where C is the normalized capacitance vector, S is the sensitivity matrix of normalized capacitance with respect to permittivity distribution, and G is a grey level vector.

There are three main challenges in ECT imaging: (1) nonlinear relationship between permittivity distribution, capacitance, and distortion of the electric field by the enclosed material —the so called soft-field effect; (2) fewer number of independent measurements compared with pixels needed to reconstruct an image; and (3) ill-posed and ill-conditioned nature of the inverse problem (Deabes and Jamil Khayyat 2021, Wang and Yang 2021). The obtained solution is often sensitive to measurement errors and noise, and therefore unstable. To obtain meaningful reconstruction results, some prior information or constraints need to be added on the unknown variables.

Various methods have been proposed to solve the ECT inverse problem within the last three decades. In general, they can be categorized into two groups, single step and iterative methods (Hussain et al. 2023, Wang and Yang 2021). Single step methods use a single mathematical step to calculate the permittivity distribution from the measured capacitance and the sensitivity matrix while iterative methods optimize a set of objective functions iteratively until steady conditions are attained.

Iterative Image Reconstruction in ECT

ECT image reconstruction involves finding the permittivity distribution from a set of measured capacitance values. Due to the non-linear relationship between measured capacitance and permittivity distribution, iterative reconstruction methods are often used to obtain better image reconstruction results. For using iterative methods to be suitable in image reconstruction, fast forward solver functionals are needed. This is because, in iterative methods, the reconstructed image is updated by minimizing the error between the measured capacitance data and the forward solution for a given permittivity distribution. This process is repeated iteratively until a pre-defined criterion is met; hence a number of forward solutions is needed.

Iterative image reconstruction methods are classified into two basic categories (Deabes and Jamil Khayyat 2021): (1) algebraic reconstruction methods, in which the image is updated to minimize the error between measured capacitance and the forward solution for a reconstructed image; and (2) optimization methods, in which a set of objective functions are optimized to meet certain image constraints. In both cases, the minimization of the error based on the measured capacitance depends on the gradient of the forward solution. The update equation is expressed as

$$G_{k+1} = G_k - \beta F(G_k), \quad (6)$$

where G_{k+1} is the image vector at $(k+1)^{th}$ iteration, β is a relaxation factor, and $F(G_k)$ is the gradient of the error between forward solution for the image vector at the k^{th} iteration and the measured capacitance vector.

Techniques for addressing the forward problem, can be grouped into two main categories, namely numerical and linearization techniques. Numerical techniques include finite elements, boundary elements, and finite differences (Hasanoğlu and Romanov 2017, Nachaoui et al. 2021). These methods are more accurate; however, they are time-consuming, and hence linearization techniques are preferred for online applications. The most common linearization method is called linear forward projection (LFP), based on the sensitivity model. The sensitivity model is based on the superposition of individual pixel and the forward solution is obtained as a linear sum of capacitance values obtained from small perturbations in permittivity distribution.

Based on this model, the update equation (4) is approximated as

$$G_{k+1} = G_k - \beta S^T(C - SG_k), \quad (7)$$

where C is the measured capacitance vector, and S is the sensitivity matrix. Because of the non-linear nature of ECT, linearization techniques generate images with poor spatial resolutions. An improvement in the iterative reconstruction process can be achieved by integrating a non-linear forward solver, such that

$$G_{k+1} = G_k - \beta S^T\big(C - y(G_k)\big), \quad (8)$$

where $y(G_k)$ is the non-linear forward solution of the image vector, G_k. The reconstruction technique in this case is referred to as an iterative semi-linear back projection (Yang et al. 2023). Due to the ill-posedness nature of the ECT inverse problem, optimization techniques are more superior over algebraic reconstruction. This adds a challenge to the reconstruction problem when computational and experimental noise are present. In this case, finding the solution based solely on minimization of the forward error function (algebraic reconstruction) does not guarantee an optimum solution. However, the hybrid model which combine algebraic reconstruction for inverse problem and logistic forward solver for forward problem may provide better reconstruction results. In this work, the logistic regression forward solver is integrated into the iterative linear back projection technique, and the combination is called Iterative Linear Back Projection and Logistic Forward Solver (ILBP-LFS)

Logistic Forward Solver

In this work, a new forward solver for the ECT problem has been introduced, and integrated with iterative linear back projection reconstruction technique to address the ECT inverse problem. The forward solver is based on logistic optimization by regulating sensitivity variations between measured and calculated capacitance data. The logic solver employs the logistic regression functional which is normally used to predict a categorical variable from a set of predictor variables. With a categorical dependent variable, discriminant function analysis is usually employed if all of the predictors are continuous and nicely distributed; logistic analysis is normally applied if all of the predictors are categorical; and logistic regression is often chosen if the predictor variables are a mixture of continuous and categorical variables and/or if they are not nicely distributed —it makes no assumptions about the distributions of the predictor variables (Rymarczyk et al. 2019, 2020, 2021). The predicted dependent variable is a function of the probability that a particular subject will be in one of the categories (for example, the probability that multiphase flow contains either gas or oil or both, given its set of scores on the predictor variables). The fundamental mathematical concept underpinning logistic regression is the logit defined by

$$\log_e\left(\frac{p(G_k;\theta)}{1-p(G_k;\theta)}\right) = \theta G_k. \quad (9)$$

Equation (9) can be rearranged to give

$$\frac{p(G_k;\theta)}{1-p(G_k;\theta)} = exp(\theta G_k). \quad (10)$$

This can be simplified to

$$p(G_k;\theta) = \frac{1}{1+\exp(-\theta G_k)}, \quad (11)$$

where $p(G_k;\theta)$ represents probability of occurrence of a grey value, G_k, given optimization parameter, θ, which represents permittivity variation. The challenge is to find the value of θ which provides an optimal value of G_k.

Parameters Estimation

Because logistic regression predicts probabilities, rather than just classes, it can be approximated using likelihood (Brown 2014, Hosmer Jr et al. 2013). For each training data-point, there is a vector of features, G_k, and an observed class, y_k. The probability of the observed class is either p (for oil) if $y_k = 1$, or $(1 - p)$ (for gas) if $y_k = 0$. The likelihood is then

$$L(\theta) = \prod_{k=1}^{n} p(G_k)^{y_k}\big(1 - p(G_k)\big)^{1-y_k}, \quad (12)$$

where θ represents permittivity variation parameter. The maximum likelihood estimates the values for θ that maximizes the likelihood function in equation (15). Critical points (maxima and

minima) occur when the first derivative equals zero. If the second derivative evaluated at that point is less than zero then the critical point is maximum. Thus, finding the maximum likelihood estimates requires computing the first and second derivative of the likelihood function. Taking the derivative of equation (15) with respect to θ is a difficult task due to the complexity of the multiplicative terms in equation (15). The log-likelihood function for the logistic regression model is given by:

$$l(\theta) = \sum_{k=1}^{n}\left(y_k \log p\,(G_k) + (1 - y_k)\log\left(1 - p(G_k)\right)\right). \quad (13)$$

Rearranging this equation we have

$$l(\theta) = \sum_{k=1}^{n}\log\left(1 - p(G_k)\right) + \sum_{k=1}^{n} y_k \log\left(\frac{p(G_k)}{1-p(G_k)}\right). \quad (14)$$

by substituting equations (10) and (11) into this rearranged equation, we get:

$$l(\theta) = -\sum_{k=1}^{n}\log(1 + \exp(-\theta G_k)) + \sum_{k=1}^{n} y_k(\theta G_k). \quad (15)$$

To find maximum likelihood estimate, we differentiate this log-likelihood function with respect to θ , set the derivatives equal to zero, and solve:

$$\frac{\partial l}{\partial \theta_j} = -\sum_{k=1}^{n}\frac{G_{kj}\exp(-\theta G_k)}{1+\exp(-\theta G_k)} + \sum_{k=1}^{n} y_k\, G_{kj} \quad (16)$$

Using the Newton-Raphson method for numerical optimization, this derivative is solved iteratively by:

$$\theta^{(n+1)} = \theta^{(n)} - \frac{f'(\theta^{(n)})}{f''(\theta^{(n)})}. \quad (17)$$

Once the optimization parameters have been obtained, the forward solver $y(G_k) = C_i^{calc}$ given in equation (8) is updated by the non-linear forward logistic solver using

$$C_i^{calc} = \frac{\sum_{J=1}^{N} S_{ij}G_j}{1+\exp\left(-\theta\sum_{J=1}^{N} S_{ij}G_j\right)},\ \text{i=1,2,3…,M,} \quad (18)$$

where M and N are respectively total numbers of measurements and pixels. Hence the new grey values are calculated iteratively using

$$G_{k+1} = G_k - \beta S^T(C^{meas} - C^{calc}), \quad (22)$$

where β is a relaxation factor, and k represents k^{th} iteration, C^{meas} and C^{calc} are respectively measured and calculated capacitances. The flow of execution of the proposed algorithm is given in Figure 1.

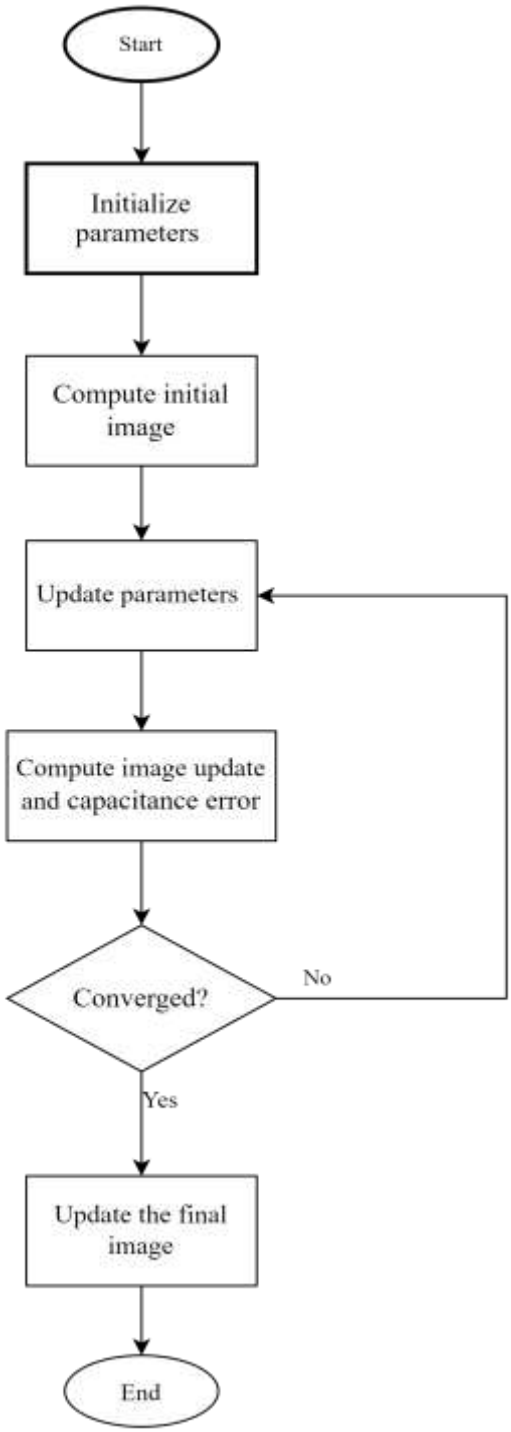

Figure 1: Flowchart for Iterative Linear Back Projection and Logistic Forward Solver

Experimental Setup and Evaluation Criteria

In order to evaluate the efficacy of the proposed method, experiments were carried out using an 8-electrode circular sensor ECT system (excitation waveform: 10Vpp, 300-500kHz), with sensing domain divided into 900 pixels with 32×32 grid (Figure 2). Static experiments were conducted using annular and stratified perspex beads positioned at different locations in the sensing domain. Simulated capacitance data were used to analyse performance of the proposed method over full component fraction range. All reconstruction methods were implemented using MATLAB on a computer with Intel Core i7-4510U CPU, @ 2 GHz, 2GHz, and 8.00GB memory.

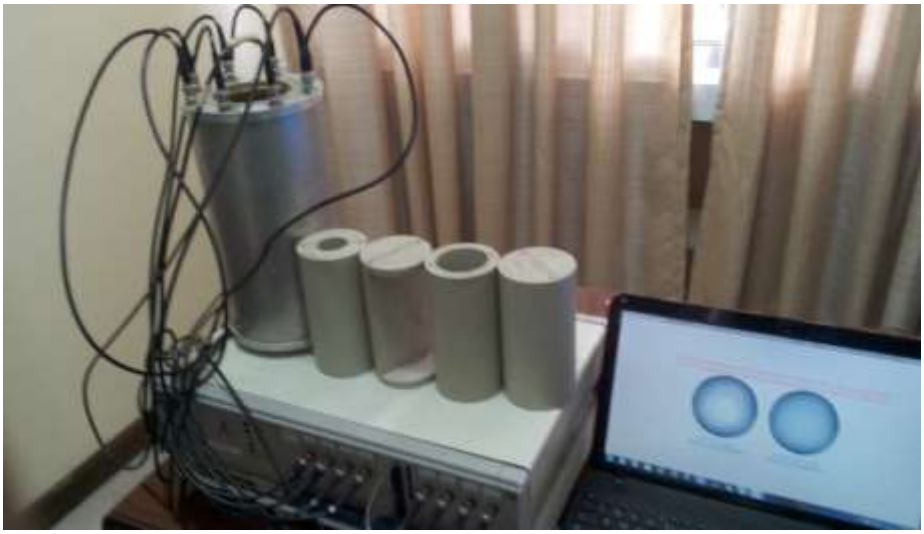

Figure 2: An 8-electrode sensor ECT system at the University of Dar es Salaam.

Qualitative and quantitative evaluations were made between the new method (ILBP-LFS), ILBP and PLAND methods. ILBP and PLAND have been used in evaluation of the proposed method because they generate better images and have higher spatial metric performance than other methods. In addition, these are the widely used methods for commercial and research applications. Qualitatively, visual results of the reconstructed images generated by different methods were subjectively compared. To quantify the results, distribution error (DE), relative image error (RIE) and correlation coefficient (CC) metrics, were used to compare the spatial resolution between the reference and the reconstructed images. Lower DE and RIE and higher CC values signal better results; for reservoir management in oil industries, for example, the desired DE should be less or equal to 10%.

Results and Discussions

Figure 3 presents qualitative visual inspection results from image generated using ILBP, PLAND and ILBP-LFS reconstruction methods. Results show that the proposed ILBP-LFS method generates sharper and detailed image compared with PLAND and ILBP. The proposed algorithm is accurate relative to its counterpart methods. However, the proposed algorithm also fails to resolve bubble flow, unless thresholding is applied.

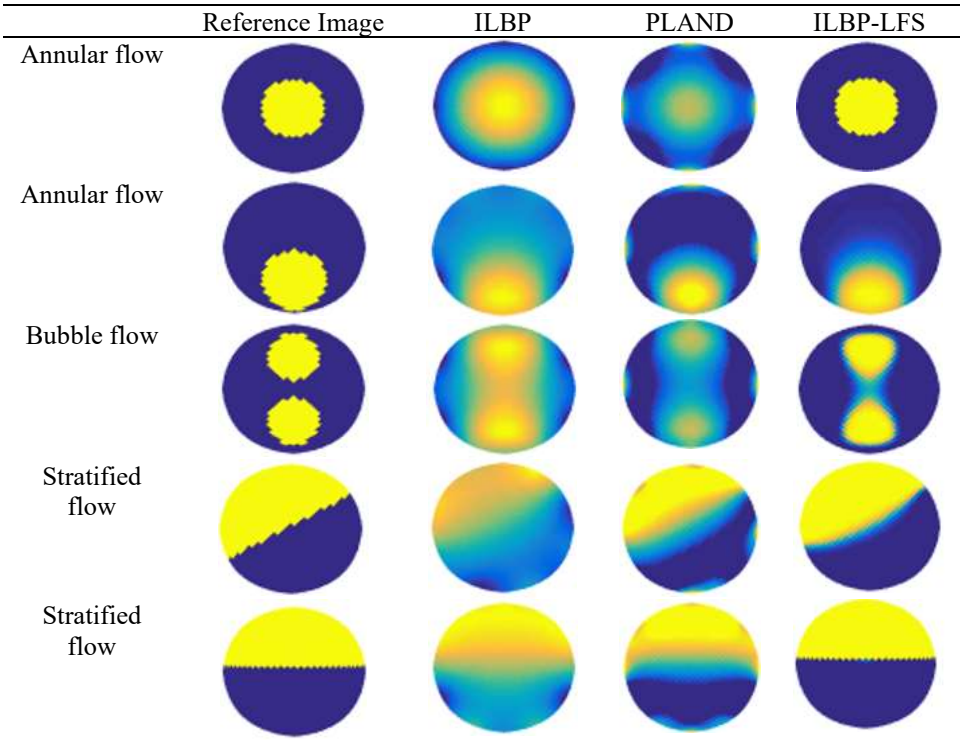

Figure 3: Images reconstructed using simulated experimental data

The evaluation was extended to cover the full component fraction range for annular and stratified flows. Figure 4 presents quantitative results based on distribution error (DE) similarity quality metric for ILBP, PLAND and ILBP-LFS methods over full component fraction range for annular flow. It is noted that ILBP-LFS is significantly more accurate compared with other methods. Its average DE over full component fraction range is below 10% suggesting that ILBP-LFS can be used for commercial application in oil industries.

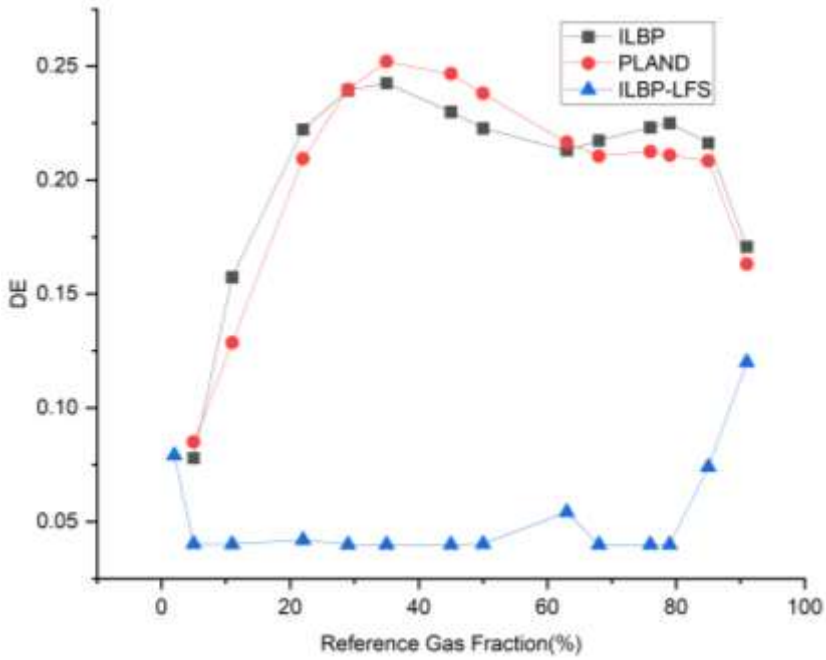

Figure 4: DE for annular flow over full component fraction range

In Figure 4, the DE performance results for ILBP, PLAND, and ILBP-LFS methods for stratified flows over full component fraction range are presented. Again, ILBP-LFS performs better than ILBP and PLAND over full component fraction range, giving an average DE of less than 10%. At lower and higher gas concentration, ILBP-LFS performs better with lower DE values. This is caused by lower permittivity variations in the sensing domain. When reference gas fraction is approximately 50%, the performance of ILBP-LFS decreases because of high change in permittivity variation, but the overall DE is less than 10% over full component fraction range.

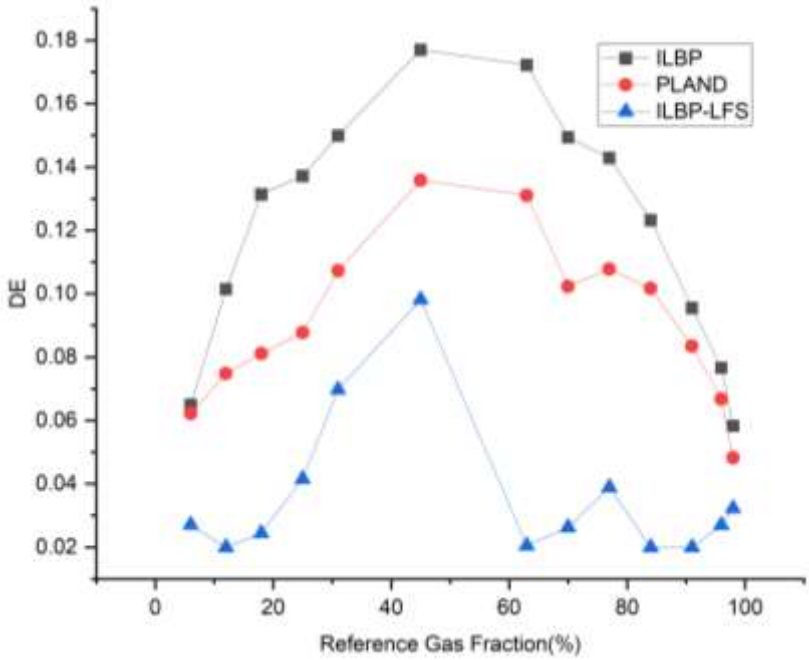

Figure 5: DE for stratified flow over full component fraction range

Table 1 presents average numerical results for ILBP-LFS, PLAND, and ILBP methods for annular and stratified flows (Figures 4 and 5). ILBP-LFS has lower values of DE, and higher value of CC compared with PLAND and ILBP. This observation signals better accuracy performance of the ILBP-LFS method. These numerical results agree with the visual analysis, suggesting that the ILBP-LFS method has better accuracy performance compared with PLAND and ILBP. To compare the execution speed, reconstruction time was also recorded for each method using single frame image data. From Table 1, it can be seen that ILBP-LFS is computationally efficient compared with PLAND and ILBP methods.

Table 1: Quantitative evaluation using RIE, DE and CC

Method	DE (%)		CC		Time (sec)
	Annular	Stratified	Annular	Stratified	
ILBP	27.42	15.75	0.662	0.845	0.068
PLAND	24.18	12.14	0.745	0.895	1.98
LFS-LFS	17.98	7.249	0.766	0.894	0.028

The experiment performance evaluation the proposed algorithm showed that the algorithm significantly improve accuracy relative to its established counterpart algorithms. This observed performance has been consistent for both qualitative visual inspection and quantitative evaluation using similarity quality metrics. The accuracy performance of less than 10 % is desirable in some of industrial applications for operation purposes.

A desirable reconstruction algorithm performance should be flow-regime independent and consistent over full component fraction range. The evaluation of different flow regimes, bubble, annular and stratified flows over full components demonstrated the consistent accuracy

performance of the proposed algorithm. In this case it constitutes robustness of the algorithm which is superior over its counterparts evaluated in this work.

The computation inefficiency of the iterative reconstruction algorithm is one of the challenges of interest to researchers. Improving it has been the objective of new proposed algorithms. In this study, it was demonstrated that the ILBP-LFP implementation improved the computation efficiency relative to its counterpart's algorithms. The algorithm has improved the speed of reconstruction to 59 % of the basic ILBP reconstruction algorithm.

Conclusion

In this paper, a new forward solver for the ECT problem has been introduced, and integrated with iterative linear back projection reconstruction technique to address the ECT inverse problem. The forward solver is based on logistic optimization by regulating sensitivity variations between measured and calculated capacitance data. The image update is performed by minimizing the error of the predicted capacitance based on grey value fitting of the logistic solver. The new image update technique overcomes instability problems usually faced in implementing sensitivity models for image reconstruction. An improvement in reconstructed images is also verified using the non-linear update when compared to linear techniques such as projected Landweber and iterative linear back projection. The proposed technique is fast and can be easily integrated into any iterative reconstruction method.

References

Brown JD 2014 Maximum-Likelihood Estimation. In *Linear Models in Matrix Form* (pp. 69–104), Springer International Publishing, Cham.

Chowdhury SM, Marashdeh Q, Teixeira FL, and Fan LS 2022 Electrical Capacitance Tomography. *Industrial Tomography: Systems and Applications, Second Edition* (pp. 3–29), Woodhead Publishing, Cambridge.

Deabes W and Jamil Khayyat KM 2021 Image reconstruction in electrical capacitance tomography based on deep neural networks. *IEEE Sens. J.* 21(22): 25818–25830.

DeMaris A and Selman SH 2013 Logistic Regression. In *Converting Data into Evidence* 115–136. Springer New York, New York, NY.

Dimas C, Alimisis V, Uzunoglu N, and Sotiriadis P 2024 Advances in Electrical Impedance Tomography Inverse Problem Solution Methods: From Traditional Regularization to Deep Learning. *IEEE Access*. 12: 47797–47829.

Hasanoğlu AH and Romanov VG 2017 Introduction to inverse problems for differential equations, Springer International Publishing, Cham.

Hong Q, Lai MJ, and Wang J 2021 The convergence of a numerical method for total variation flow. *JACT*. 15.

Hosmer JR D, Lemeshow S, and Sturdivant R 2013 Applied logistic regression, John Wiley & Sons.

Hussain A, Faye I, Muthuvalu MS, Tang TB, and Zafar M 2023 Advancements in Numerical Methods for Forward and Inverse Problems in Functional near Infra-Red Spectroscopy: A Review. *Axioms.* 12(4): 326–348.

Li J, Tang Z, Zhang B, and Xu C 2023 Deep learning-based tomographic imaging of ECT for characterizing particle distribution in circulating fluidized bed. *AlChE J.* 69(5): e18055.

Nachaoui A, Nachaoui M, Chakib A, and Hilal MA 2021 Some novel numerical techniques for an inverse Cauchy problem. *J. Comput. Appl. Math.* 381:113030.

Rajan MP and Jose J 2022 An Efficient Discrete Landweber Iteration for Nonlinear Problems. *Int. J. Appl. Comput. Math*. 8(4): 1–19.

Rymarczyk T, Kozłowski E, Kłosowski G, and Niderla K 2019 Logistic Regression for Machine Learning in Process Tomography. *Sensors.* 19(15): 3400.

Rymarczyk T, Kozłowski E, Tchórzewski P, Kłosowski G, and Adamkiewicz P 2020 Applying the logistic regression in electrical impedance tomography to

analyze conductivity of the examined objects. *JAE.* 64(S1): S235–S252.

Rymarczyk T, Niderla K, Kozłowski E, Król K, Wyrwisz JM, Skrzypek-Ahmed S, and Gołąbek P 2021 Logistic Regression with Wave Preprocessing to Solve Inverse Problem in Industrial Tomography for Technological Process Control. *Energies*. 14(23): 8116.

Wajman R 2021 The concept of 3D ECT system with increased border area sensitivity for crystallization processes diagnosis. *SR*. 41(1): 35–45.

Wang H and Yang W 2021 Application of electrical capacitance tomography in pharmaceutical fluidised beds – A review. *Chem. Eng. Sci*. 231: 116236.

Yang Y, Liu J, and Liu G 2023 Image reconstruction for ECT based on high-order approximate sensitivity matrix. *Meas. Sci. Technol*. 34(9): 095402.

Zheng J and Peng L 2020 A Deep Learning Compensated Back Projection for Image Reconstruction of Electrical Capacitance Tomography. *IEEE Sens. J*. 20(9): 4879–4890.